A UNIVERSAL SYSTEM TO DE-ORBIT SATELLITES AT END OF LIFE

Juan R. SANMARTIN, Mario CHARRO, Xin CHEN
Universidad Politécnica de Madrid, Madrid, Spain

Enrico C. LORENZINI, Giacomo COLOMBATTI, Denis ZANUTTO
Università degli Studi di Padova, Padova, Italy

Jean-Francois ROUSSEL, Pierre SARRAILH
ONERA, Toulouse, France

John D. WILLIAMS, Kan XIE, Garrett E. METZ
Colorado State University, Fort Collins, CO, United States

Jose A. CARRASCO, Francisco GARCIA-DE-QUIROS
Embedded Instruments and Systems S.L., Elche, Spain

Olaf KROEMER, Roland ROSTA, Tim van ZOEST
DLR German Aerospace Center, Bremen, Germany

Joseba LASA, Jesús MARCOS
Fundación Tecnalia, San Sebastián, Spain

juanr.sanmartin@upm.es

Abstract

A 3-year Project financed by the European Commission is aimed at developing a universal system to de-orbit satellites at their end of life, as a fundamental contribution to limit the increase of debris in the Space environment. The operational system involves a conductive tape-tether left bare to establish anodic contact with the ambient plasma as a giant Langmuir probe. The Project will size the three disparate dimensions of a tape for a selected de-orbit mission and determine scaling laws to allow system design for a general mission. Starting at the second year, mission selection is carried out while developing numerical codes to implement control laws on tether dynamics in/off the orbital plane; performing numerical simulations and plasma chamber measurements on tether-plasma interaction; and completing design of subsystems: electron-ejecting plasma contactor, power module, interface elements, deployment mechanism, and tether-tape/end-mass. This will be followed by subsystems manufacturing and by current-collection, free-fall, and hypervelocity impact tests.

1. Introduction

BETs (*Propellantless deorbiting of space debris by bare electrodynamic tethers*) is a 3-year Project started on November 1, 2010, financed by the European Commission within the FP-7 Space Program, and aimed at developing an efficient de-orbit system that could be carried on board any future satellite launched into Low Earth Orbit. A dedicated system is needed because satellites naturally orbit at ionospheric altitudes where air drag is very weak. The operational system will deploy a conductive thin-tape bare-tether to collect electrons as a giant Langmuir probe, using no propellant and no power supply, and generating power on board.

The system considered involves magnetic drag on current flowing along the tether. Like air drag, magnetic drag is a dissipative mechanism arising from the orbiting-tether motion relative to the co-rotating magnetized plasma, which induces a so-called motional electric field $\overline{E}_m$ at the ambient plasma, in the frame of the tether. That field drives current into the tether, and the geomagnetic field then exerts a Lorentz force on the current-carrying tether.

Tether drag is passive like air drag and propulsive like rockets and electrical thrusters. It beats alternative systems (enhanced air drag, and rocket and electrical thrust) in simplicity and the combined basic metrics: Frontal Area x De-orbit Time and System-to-Satellite mass ratio. The project will carry out a detailed system design for a selected de-orbit mission, but scaling laws will also be determined to extend the design to a variety of missions. The Project will not address mitigation or surveillance programs, or debris already accumulated in space.

2. Need for Scaling Laws in System Design

The basic mission parameters are satellite mass M_{sat}, orbit inclination i, and initial altitude H. A vanishing eccentricity is a good approximation for almost all missions of interest; then H determines the initial orbital velocity v_{orb}. Also, taking a standard final operational altitude, 150-200 km, say, determines the altitude drop ΔH, leading to a velocity increase

$$\Delta v_{orb} \approx \sqrt{\frac{GM_E}{R_E}} \times \frac{|\Delta H|}{2R_E} \approx v_{orb} \times \frac{|\Delta H|}{2R_E}, \qquad (1)$$

where M_E and R_E are Earth mass and radius. Satellite mass, and thus mission impulse $M_{sat}\Delta v_{orb}$, presents a broad range of values affecting de-orbit time, which is sensitive to orbital inclination too.

Tether performance is also ambience dependent, ambience itself being dependent on day/night, Solar max/min conditions. Basic ambience parameters are magnetic field $\boldsymbol{B}$, plasma density n_e, ion and electron temperatures T_i, T_e, and dominant ion-species mass m_i (O^+ at the lower altitudes of interest, H^+ around 1000 km). They determine in particular the Debye length $\lambda_D \equiv \sqrt{\varepsilon_0 kT_e / e^2 n_e}$, electron thermal gyroradius $l_e \equiv \sqrt{kT_e m_e} / eB$, ion ram energy with respect to the tether $\frac{1}{2} m_i v_{orb}^2$, and motional field $\overline{E}_m \equiv \overline{v}_{orb} \wedge \overline{B}$ (neglecting the corotation velocity, which is about $v_{orb}/16$ in LEO). In turn, the debris flux environment would, in principle, be critical to mission success, published estimates suggesting a high probability of a round tether being cut by debris.

NASA tethers TSS(*Tethered Satellite System*)1, TSS1R were fully insulated round wires that carried anodic and cathodic contactors at the corresponding ends (Ref.1). The cathodic device was a Hollow Cathode, a type of highly efficient, electron ejecting Plasma Contactor. The anodic contactor was a large spherical conductor of radius 0.8 m, which is very large compared to both $\lambda_D \sim 3 - 9$ mm and $l_e \sim 3$ cm typically. This makes the sphere highly inefficient in collecting ambient electrons.

The *bare tether* concept was introduced in the early 90's (Ref.2). The tether itself, left uninsulated, was to collect electrons in the 2D-OML (*orbital motion limited*) regime over some segment coming out positively biased. A characteristically small tether diameter ~ 1 mm allows efficient collection in cylindrical geometry. In turn, a large tether length L provides a big collecting area. The 2D OML current-collection rate is proportional to L, to the perimeter of cross section p, and to the square root of bias energy $e\Delta V >> \frac{1}{2} m_i v_{orb}^2$ and kT_e. With bias varying along the tether, the average collection rate is the rate at a fraction of maximum bias.

A fundamental result from Langmuir probe theory shows that OML current collection is the same for all non-concave cross sections of equal perimeter (Ref.3). Consider now a thin-tape tether of width w and thickness $h << w$, and a 'corresponding' round tether of equal length and mass, and so equal cross-section area A. It will then have a radius $R = \sqrt{wh/\pi}$. The respective perimeters are $2w$ and $2\pi R$. Collection will thus be much greater for the tape due to the large factor $\sqrt{w/\pi h}$.

Actually, the current inside the tether is limited by ohmic effects. For such dominant effects, the length-averaged tether current I_{av} approaches the short-circuit value, $\sigma_c E_m A$ (σ_c being electric conductivity and E_m being motional-field component along the tether), which is the same for corresponding round and tape tethers, the tape having lost its perimeter advantage. But dominant ohmic effects require the condition $L >> l^{1/3} (2A/p)^{2/3}$, where l is certain ambience-dependent characteristic length,

$$l \equiv \frac{9\pi^2}{128} \frac{m_e \sigma_c^2 E_m}{e^3 n_e^2} . \qquad (2)$$

The ratio $2A/p \equiv h$ for the tape is much smaller than $2A/p \equiv R$ for its corresponding round wire; typically the ohmic-dominated limit is not reached by the wire.

A tape is characterized by 3 disparate lengths, L, w, h. While the project will carry out a detailed design for maximum performance in a specific mission, scaling laws are required to extend the optimum design to the variety of mission parameters. Such laws require an analysis of how length, width and thickness enter into multiple parameters and effects (Ref.4):

Tether mass m_t and deorbit time t_d;
Survivability;
Current response (dependent on bare-tether collection impedance Z_{coll}, ohmic resistance R_Ω, useful load impedance Z_{Load}, and impedance for tether wave emission);
Thermal response;
Tether bowing;
Magnetic effects on collection from both the ambient field $\boldsymbol{B}$ and the self-field from tether current itself;
Special collection effects both anodic (adiabatic electron trapping) and cathodic (thermionic emission from low Work-function coating).

3. Limits on Tether-to-satellite Mass Ratio and De-orbit Time

Some effects on collection, such as due to the ambient magnetic field, may affect tapes more than corresponding round tethers. However, as regards the critical issue of survivability of a tether itself against debris flux, a tape is highly favoured. Use of a tape, as opposite use of its corresponding round tether, reduces considerably the total fatal-impact count because both *i*) de-orbit time t_d and *ii*) fatal-impact rate are reduced. Fatal-impact count may be smaller for the tape by more than two orders of magnitude. Reduction *i*) arises from the already noticed greater collection capability of the tape. Reduction *ii*) arises from the much lower fatal-debris flux at the large front area presented by the tape except for near edgewise impacts, for which the very small debris to consider bring too little energy to cut the tether throughout most of its width. An approximate average expression for the number of fatal impacts during de-orbiting, using NASA's ORDEM model (*Orbital Debris Engineering Model*, Ref.5) is

$$N_c \sim \frac{99}{\sqrt{4\pi}} \sqrt{\frac{w}{h}}\, wL \times F(w) \times t_d \qquad (3)$$

where $F(w)$ is cumulative debris flux covering debris size larger than w (Ref.6).

From Poisson's distribution, the condition for a high probability of survival during de-orbiting reads $exp(-N_c) \approx 1$, or $N_c << 1$. Using representative values w = 20 mm, h = 0.05 mm, L = 10 km, and F(20 mm) ~ 10^{-5} /m^2× year in NASA's ORDEM, for H = 800 km and i = 28.5°, the small N_c condition gives

$$t_d << 10.7 \text{ months.} \tag{4}$$

The de-orbit time can be obtained from the averaged mission-impulse equation,

$$M_{SC}\,\Delta v_{orb} = LI_{av}\bar{u} \wedge \bar{B} \cdot \frac{-\bar{v}_{orb}}{v_{orb}} \times t_d = \tilde{I}_{av} L \sigma_c E_m^2 wh \times t_d / v_{orb} \tag{5}$$

with the tether assumed vertical, along the gravity gradient, and $\bar{u}$ being the vertical unit vector (upwards for $i < 90°$), and where we introduce a normalized length-averaged current

$$\tilde{I}_{av}\left[\frac{L}{l^{1/3}(2A/p)^{2/3}}\right] \equiv \frac{I_{av}}{\sigma_c E_m wh}. \tag{6}$$

Note that the motional field can also be written as $E_m = \bar{u} \wedge \bar{v}_{orb} \cdot \bar{B}$. Since $\bar{u}$ and $\bar{v}_{orb}$ are perpendicular to each other, the ratio E_m/v_{orb} is the magnetic field component $B_\perp$ perpendicular to the orbital plane. Detailed de-orbit calculations using both off-center dipole and multipole geomagnetic-field (IGRF-11) models, and $\tilde{I}_{av}$ = 1 for simplicity, do show de-orbiting slowest around 85° inclination, the increase in t_d from its value at low inclination corresponding to a decrease in E_m^2 in Eq.(5) by a factor of about 20 (Ref.7).

Eliminating t_d between (3) and (5) the small N_c condition reads

$$\frac{m_t}{M_{SC}} >> \frac{\rho v_{orb}\Delta v_{orb}}{\tilde{I}_{av}\sigma_c E_m^2} \times \frac{99}{\sqrt{4\pi}}\sqrt{\frac{w}{h}}\, Lw \times F(w) \tag{7}$$

where ρ is tether density. Setting $|\Delta H|$ = 650 km and $\rho/\sigma_c E_m^2$ = 3.5 kg/kW (for aluminum and low inclination) we find

$$\frac{m_t}{M_{sat}} >> \frac{0.36}{\tilde{I}_{av}} \times 10^{-3}. \tag{8}$$

Opposite limits on mass ratio and de-orbit time result from requiring that at given mission impulse a tether be much more efficient than, say, a rocket. System-to-mission impulse ratio for rocket and tether can be written, respectively, as

$$\frac{rocket\ system\ mass}{mission\ impulse} \approx \frac{\dot{m}\Delta t}{\dot{m} c_{ex}\Delta t} = \frac{1}{c_{ex}}, \tag{9}$$

$$\frac{tether\ system\ mass}{mission\ impulse} \approx \frac{\alpha\, m_t}{M_{sat}\Delta v_{orb}}, \tag{10}$$

where $\dot{m}$ and c_{ex} are rocket mass-flow-rate and exhaust velocity respectively, and a factor $\alpha \sim 2$ accounts in particular for tether-deployer mass. We then require that the tether-to-rocket system-mass ratio be small, or equivalently,

$$\frac{m_t}{M_{sat}} << \frac{\Delta v_{orb}}{\alpha\, c_{ex}} \approx 0.68 \times 10^{-1}, \tag{11}$$

where we used c_{ex} = 2.8 km/s for a solid-fuel rocket. Finally, taking m_t/M_{sat} from (5) we find

$$t_d >> \frac{\alpha}{\tilde{I}_{av}}\frac{\rho}{\sigma_c E_m^2} v_{orb}\, c_{ex} \approx \frac{1.70}{\tilde{I}_{av}}\, days \tag{12}$$

4. Dynamical Modelling

Important topics in the technological development of a system to deorbit space debris through passive electric propulsion involve the study of tether dynamics and control and the analysis of the deorbit performance. Understanding these topics requires among others the development of specialized computer codes. We have developed two new computer codes for the simulation of the dynamics, thermodynamics and electrodynamics of bare tether systems that differ mainly for the complexity in modeling the tether flexibility.

The two models utilize up-to-date versions of the environmental routines in terms of ionospheric density (IRI-2007), atmospheric density (NRLMSISE-00) and magnetic field model (IGRF-2005). The gravity field is a 4x4 model that is more than sufficient for the purpose of this study. The atmospheric and ionospheric models are particularly heavy to run on a computer and for this reason the simplified model makes use of interpolated data from those models to run more efficiently while preserving sufficient accuracy. In the simplified code the tether motion is limited to the libration dynamics and, consequently, the tether is modeled as a rigid bar. The more accurate code models the flexibility of the tether and its string dynamics through a lumped-mass model of the tether.

An extensive parametrical study of system performance led to the identification of those parameters having greater influence on de-orbiting. Another issue regards the stability of the tether dynamics during deorbiting that can be solved, for example, through tether current control. Figure 1 shows the orbit decay of a 5-km tether attached to a 1000-kg spacecraft starting at a 1000 km altitude.

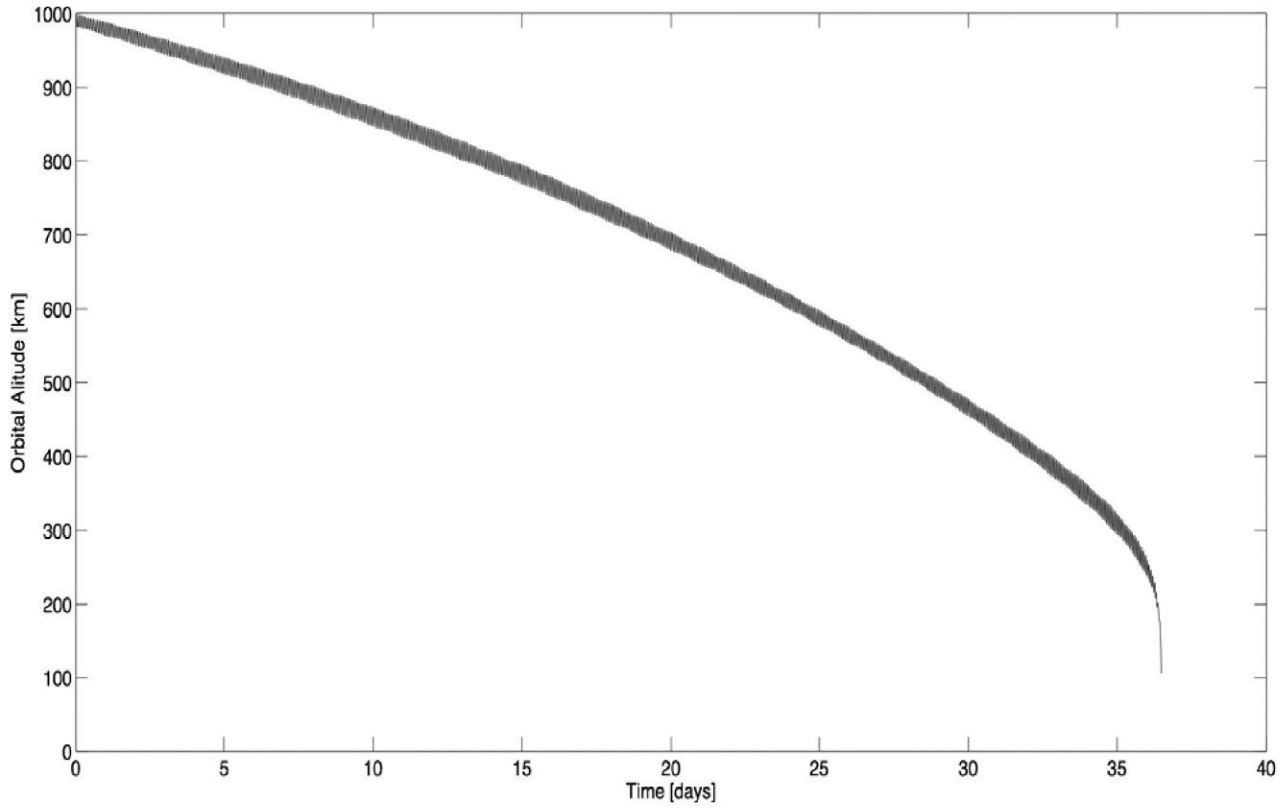

Fig. 1 Expected decay from equatorial orbit vs. time for a 5-km long, 1 cm wide, tape-tether collecting OML current; de-orbiting mass is 1000 kg.

The figure clearly shows that a relatively short tether, that is appropriately stabilized by control, can de-orbit a 1000-kg spacecraft in about a month. A heavier spacecraft will de-orbit in a time inversely proportional to its mass. De-orbit times are very short considering the recommendation that

requires a satellite to de-orbit within 25 years. During the de-orbiting process, the orbit becomes slightly eccentric, making the altitude oscillate between perigee and apogee twice per orbit. There are about 1000 such oscillations over the 33 days de-orbit time, making a small scale plot look noisy.

5. Current Collection Issues

With the current loop closed through the plasma, tether-contact effectiveness on both anodic and cathodic sections is crucial. This can be expressed as a plasma impedance, or a current-tension characteristics, since it is not linear. In the BETs project, cathodic contact is ensured by a hollow-cathode plasma contactor, whereas anodic contact relies on ambient electron collection by the tether itself. Plasma flow around the anode is however in a highly non trivial regime. The relative ion flow is hypersonic, while tether bias is highly ion repelling, $kT_i << \frac{1}{2} m_i v_{orb}^2 << e\Delta V$, as already noticed. This regime induces accumulation of ions ahead of the tether, which can result in turbulence.

Our main interest yet relies in the flow of electrons in the anodic sheath, because they are carrying the current. Since there is no real analytical or semi-analytical model of this exacting regime, it is not surprising that comparison of experimental data to approximate models show no better agreement than typically a factor of two. This directly impacts on the sizing of the tethered system and needs to be improved. The physics at the origin of these discrepancies can be electron magnetization or adiabatic electron trapping (possibly related to some turbulence). The existence of slow ions created by charge exchange with residual neutrals in ground plasma tanks is also a possible source of error in that comparison.

This issue is studied in the BETs project by both experimental and theoretical approaches. This is now in progress at ONERA's Space Environment Department in Toulouse. Modeling of the plasma was performed with the SPIS code (Ref.8) using a full PIC (Particle-In-Cell) method. Figure 2 displays a 2D ion density spatial distribution, clearly showing the wake and the accumulation of ions upstream of the tether. The other ion accumulation zone, close to their injection region, is more dynamical and its behavior is still under study

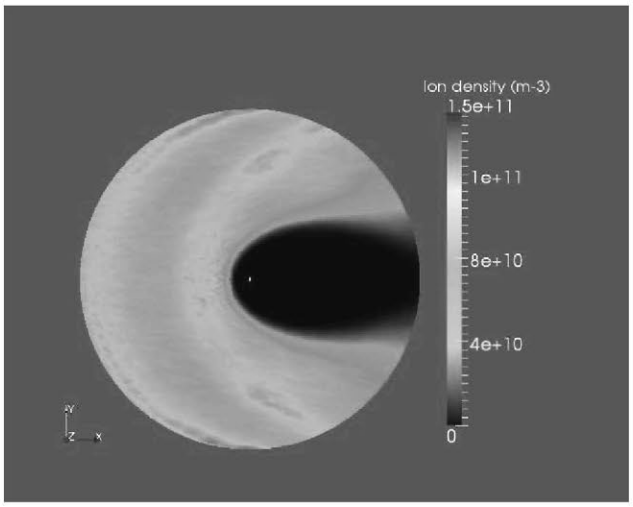

Fig. 2 PIC simulation results on ion density for tether bias $\Delta V = +50$ V, $n_e = n_i = 10^{11}$ m^{-3}, $T_e = T_i = 0.1$ eV and $v_{orb} = 8$ km/s.

Experiments were also conducted in ONERA's JONAS plasma tank (Ref.9). Special care was taken of plasma characterization since fast and slow ion populations must accurately reproduce tank conditions in simulations. Several types of Langmuir probes are used at the same location to allow

extracting both ion densities and electron parameters by computer modeling (classical Langmuir probe characteristics are not accurate enough in the present situation). A triple probe was also used for a more extensive characterization of the plasma in space and time dependent analysis. Time oscillations were observed in some regimes (at large positive probe potential) but require additional analysis.

6. Hollow Cathode Design

The plasma contactor is based on a discharge chamber that is driven by a hollow cathode as shown in Fig. 3 (Refs. 10-12). The hollow cathode is comprised of a tantalum tube that contains a low-work-function, impregnated, sintered tungsten insert. The hollow cathode tube is capped with an orifice plate on its centerline. The cathode tube and insert are heated to approximately 1100 °C by a resistive coil wrapped around the outside of the tube. The outside of the heater coal is thermally insulated with a multiple-layer, tantalum-foil radiation shield. The keeper is made of graphite and completely encloses the cathode except for an orifice located over the cathode orifice. The keeper orifice is 2.5 mm in diameter and is positioned ~1mm downstream of the cathode orifice plate.

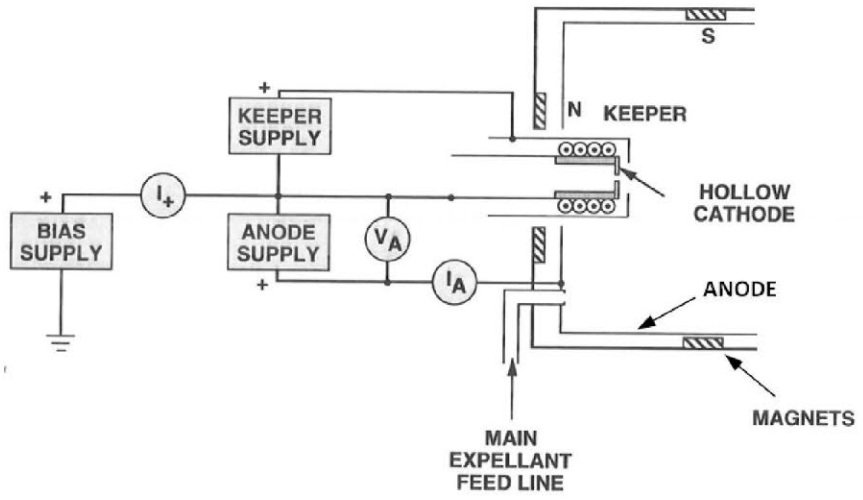

Fig. 3 Circuit schematics of plasma contactor arranged in configuration for measuring plasma ion production efficiency.

The BETS Project discharge chamber equipped plasma contactor operates with enhanced plasma production, minimum expellant flows, and minimum impedance without reliance on the space plasma properties of the orbit or day-night cycle. The discharge chamber is made from mild steel and includes two magnetic rings made of samarium cobalt located on the inside of the chamber. The first ring is located near the exit of the ion source at one end of the cylindrical side wall, and the second is placed behind the cathode on the back plate. The diameter of the discharge chamber is 10cm and the length is ~11 cm. The magnetic field magnitude at the tip of the keeper is 150 Gauss, and a 50 Gauss contour line encloses the interior of the discharge chamber, which contains the plasma and enhances the plasma ion production efficiency of the source.

Testing of the plasma contactor was performed in a 1.7 m diameter by a 4.9 m long vacuum chamber that was pumped with two 0.61 m diameter, 12 kW diffusion pumps. The base pressure of this facility with no flow is 4×10^{-6} Torr. The vacuum pressure is in the low 10^{-5} Torr range at flow rates of 3 to 10 sccm of Ar or Xe gas. Two mass flow controllers rated for 0-50 sccm and 0-200 sccm argon flow with power supply readout are used to control the cathode gas flow and main gas flow. Table 1 contains plasma ion production data at two operating conditions measured with argon and

xenon. The expellant utilization efficieny, η_u, is found by taking the ratio of the plasma ion production rate, I_+, to the total expellant flow rate measured in mAeq. Expellant utilization efficiencies of 48% were obtained on xenon, which were much higher than efficiencies obtainable with argon. The plasma ion energy cost, $\varepsilon \equiv V_A I_A / I_+$, were also found to be significantly lower for xenon. We also note that xenon is much easier to store at high density, which reduces the size of the gas storage system. These performance benefits of xenon support its use over argon, even though xenon is significantly more expensive.

Table 1. Plasma ion production measurement of hollow cathode.

Propellant	I_+ (mA)	V_A (V)	I_A (A)	η_u (%)	ε (W/A)
Argon	65	51.0	1.0	5.2	782.2
Xenon	125	31.7	1.5	48	380.1

Figure 4 contains data collected when the hollow cathode was biased negative of the vacuum chamber wall and electrons were allowed to flow from the cathode through the discharge chamber plasma and through the expanding plasma downstream of the discharge chamber to the vacuum chamber wall. Argon gas was used to operate the plasma contactor. These tests simulate how the plasma contactor will emit plasma electron current to the ionosphere in an electrodynamic tether application. Bias voltages less than 45 V were required to emit electron currents up to 4A.

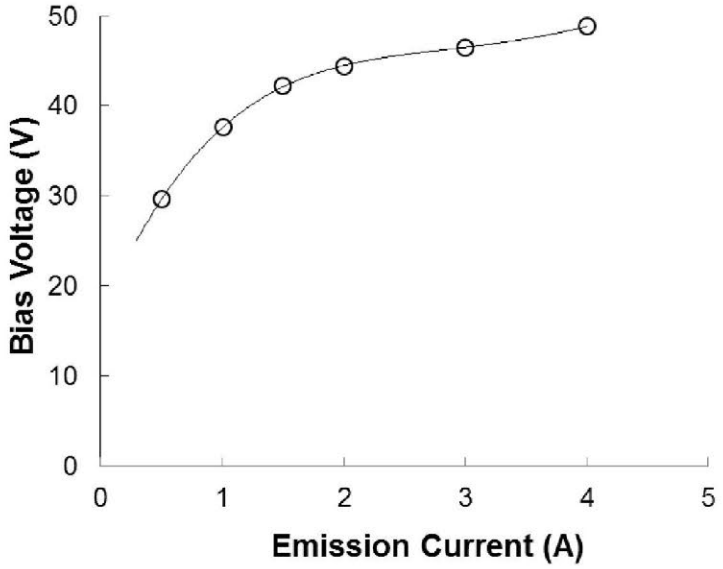

Fig. 4. Electron emission current versus bias voltage of hollow cathode for 0.52 mg/s argon gas flow and 25 W discharge power.

7. Power Control Module

The power system handles the tether-injected energy and energizes the hollow cathode during the de-orbit maneuver. It has been designed to allow autonomous operation of the complete tether-cathode system once de-orbiting is started. The system relies on a completely decentralized regulated topology (Ref.13), with all different subsystems attached to a common DC bus, to allow their full control and to readily respond to expected fast transients of the electrodynamic tether (Fig.5)

The main components of the power system are:

* A DC/DC converter that powers the DC bus while the system is not in de-orbit operation (stand-by) in order to charge a battery and have control of it through the satellite telecommand and telemetry bus (TM/TC).
* A battery that is maintained charged in order to achieve autonomous operation of the system. When the system is in stand-by, the battery is maintained in trickle charge by using a battery charge regulator (BCR) that extracts power from the DC bus. While in operation, a battery discharge regulator (BDR) maintains the voltage of the DC bus.

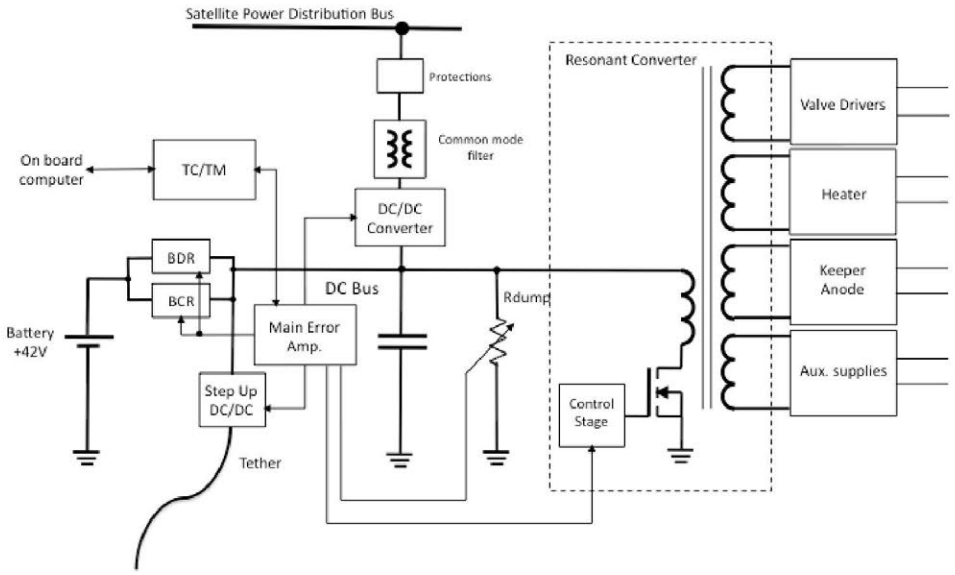

Fig. 5 Power system layout of the tether system.

* A resonant stage (Ref.14) that powers the hollow cathode with different voltages from the DC bus of the system.
* A step-up converter that gets the energy from the electrodynamic tether and injects it into the DC bus to be used for battery charging and powering the hollow cathode.
* A dump resistor that dissipates excess of energy produced by the hollow cathode while in operation.
* A main error amplifier that harmonizes the operation of all the mentioned subsystems by implementing a 3-domain control (Ref.15).

There are four working modes in the system: one occurs when the satellite is in its operational life, and thus the tether system is in stand-by, and the other three when the satellite is being decommissioned by the electrodynamic tether. The decision of being in stand-by or de-orbiting is handled by the TM/TC in coordination with the satellite on board computer (OBC). While in standby the main error amplifier operates the DC/DC converter and the BCR for maintaining the battery fully charged. While de-orbiting the main error amplifier voltage determines in which of the three operational modes is the power system working in and what subsystem is regulating the DC bus:
* Dump mode: the battery is fully charged and the tether provides more energy than needed to power the hollow cathode. The dump resistance enters into operation to dissipate the excess of power and its operation regulates the DC bus.
* BCR mode: the battery is charging from the energy provided by the tether, which supplies power to the hollow cathode as well. The BCR regulates the DC bus.
* BDR mode: the battery and the tether supply the hollow cathode because not enough power comes from the tether. The BDR regulates the DC bus in this situation.

The usual techniques for reliability and single point failure-free design allow the production of satellite flight hardware following the described topology.

8. Deployer Design

The main goal in designing the deployer was to create a completely passive unreeling mechanism that can be implemented in every satellite system without requiring big modifications. This goal can be reached with a stand-alone design in which just one signal is needed, after the satellite reaches its end of life, to start deployment of the tether. Because of this, unreeling proceeds with no control from the satellite on-board data-handling system and with no power supply.

In the first phase of the design a state-of-the-art survey, and additional theoretical investigations were carried out, to attain an overview of already existing deployers, as well as an estimate of environmental parameters influencing deployer functionality, and their effects on it. Based on DLR experience in deploying small electro conductive tethers (Ref.16) and a flat cable on planetary surfaces (Ref.17) different concepts have been developed and evaluated. Seven among those different concepts were realized in bread-board units to perform deployment tests under a variety of conditions, considering required pull force at tether release and deployment behaviour.

The result of the deployment tests show that deployment from a reel appears to less affect deployment behaviour, such as possibly leading to failure. Entanglement risk was the lowest and no tether twisting occurred. The final design of the deployer is shown in Fig.6. For the deployment of the tether the end-mass on the front will be ejected smoothly with separation springs to pull the tether from the reel. Due to both the constancy of angular momentum and the decreased tether-coil diameter, the unreeling speed increases as deployment proceeds. To ensure that tether unreeling speed does not exceed a predetermined value, a centrifugal break is set in on the rotation axis. For the connection between the tether and the hollow cathode a slip ring is used.

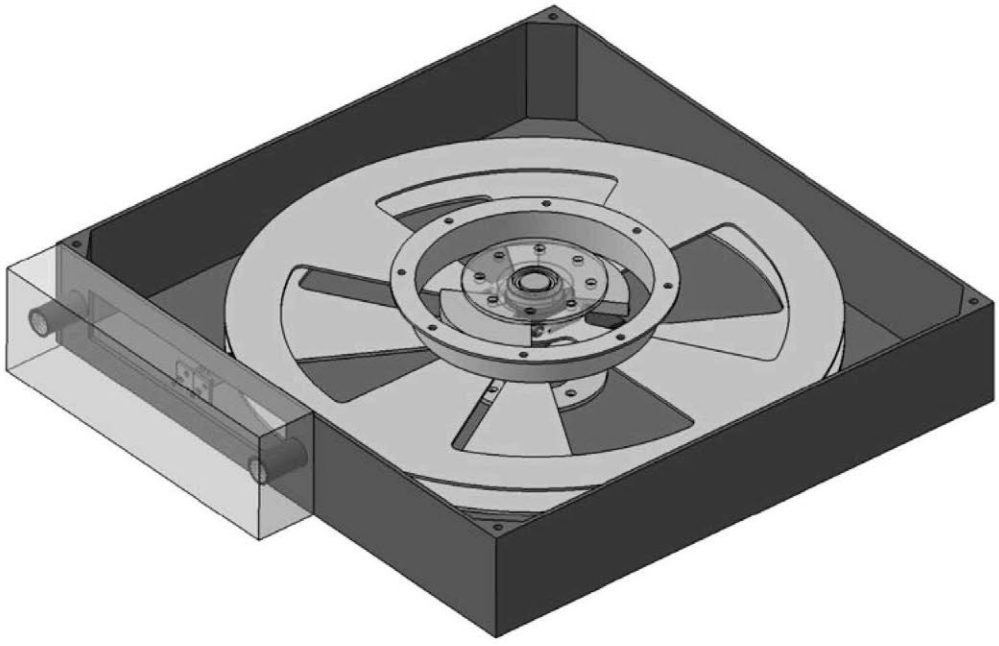

Fig. 6. Passive tether deployment mechanism. Deployer size, including the end mass, is 670mm x 710mm x 123mm. The reel is capable of holding a 6 km long tether.

Considering full scale missions with tether lengths of the order of 10 km, say, the increase in diameter of the tether reel may compromise the requirement of universal use irrespective of satellite. To overcome this drawback, the entire tether length can be distributed over several reels. In this way, the overall reel diameter can be kept in check, with just the full reel-system height increasing.

9. Tape Design

Different materials and different tether-design alternatives have been considered, in particular Hoytether and AmberStrand, and also ProSEDS (Propulsive-SEDS) and T-Rex (Tyrannosaurus-Rex), both missions intended to test bare-tether collection. ProSEDS (Ref.18) was to fly piggyback on a GPS replacement Delta-2 mission at end of March 2003, but following the Shuttle Columbia disaster two months before, ProSEDS was first placed on hold, then cancelled. T-Rex (Ref.19), a sub-orbital mission, flew on a S-520-25 JAXA rocket on August 31, 2010 and successfully deployed to 137 m.

Tentatively, a mixed tape design has been selected, involving the cross-section structure of T-Rex, and the length-wise structure of ProSEDS. As regards the cross-section structure, the tape will be made of ALPET, which comprises three different layers: two external ones, conductive and manufactured in aluminium 1350, and a core manufactured in PET, a thermoplastic polymer resin (Polyethylene terephthalate). The core would be typically 25-28 μm thick and the *Al* layers 10-12 μm thick, with tape width of the order of several centimetres.

Lengthwise the tape would be made of three segments, *A*, *B*, and *C*, like ProSEDS. The middle one, *B*, would be bare ALPET. Segment *C*, next to the satellite, would be ALPET carrying a dielectric coat to avoid possible arcing at deployer and satellite. When *C* reaches outside, the triple point junction (*B*, *C*, and ambient plasma) might support arcing in case *B* is highly negative with respect to the ambient plasma; a semiconductor sleeve at the junction would smooth the local electric field at the triple point, to suppress arcing as verified in lab tests. *A* is joined to the End-Mass and also made of ALPET, but it will not carry current, being insulated from *B*.

10. Summary

The operational system for the BETs project involves a conductive tape-tether left bare to collect electrons from the ambient plasma as a giant Langmuir probe. The Project is sizing the three dimensions of a tape for a selected de-orbit mission and will determine scaling laws to allow general mission design. During the present second year, work is carried out on developing numerical codes to implement control laws for tether dynamics in/off the orbital plane; performing numerical simulations and plasma chamber measurements on tether-plasma interaction; and completing design of subsystems: electron-ejecting plasma contactor, power module, interface elements, deployment mechanism, and tether-tape/end-mass. During the third year, will involve subsystems manufacturing and current-collection, free-fall, and hypervelocity impact tests.

Acknowledgment

Project 262972 (BETs) is financed by the European Commission under the FP7 Space Program.

References

1. Cosmo, M.L. and Lorenzini, E.C., "Tethers in Space Handbook", Smithsonian Astrophysical Observatory, Cambridge, MA, 3rd edition, 1997.
2. Sanmartin, J.R., Martinez-Sanchez, M. and Ahedo, E., "Bare Wire Anodes for Electrodynamic Tethers", J. Prop. Power **9**, 353-360, 1993.
3. Laframboise, J.G. and Parker, L.W., "Probe Design for Orbit-limited Current Collection", Phys. Fluids **16**, 629-636, 1973.
4. Sanmartin, J.R., Lorenzini, E.C. and Martinez-Sanchez, M., "Electrodynamic Tether Applications and Constraints", J. Space. Rockets **47**, 442-456, 2010.

5. The New NASA Orbital Debris Engineering Model ORDEM2000, NASA/TP-2002-210780.
6. Khan, S.B. and Sanmartin, J.R., "A Comparison of Probability of Survival for Round and Tape Tethers against Debris Impact", J. Spacecraft and Rockets, submitted.
7. Bombardelli, C., Zanutto, Denis, and Lorenzini, E.C., "De-orbiting Performance of Bare Electrodynamic Tethers in Inclined Orbits", J. Guidance, Control and Dynamics, submitted.
8. Roussel, J-F., Rogier, F., Dufour, G., Matéo-Vélez, J-Ch., Forest, J., Hilgers, A., Rodgers, D., Girard, L. and Payan, D., "SPIS Open Source Code: Methods, Capabilities, Achievements and Prospects", IEEE Trans. Plasma Sci. **36**, 2360-2368, 2008.
9. Matéo-Vélez, J-Ch., Roussel, J-F., Sarrailh, D., Boulay, F., Imguimbert, V., and Payan, D., "Ground Plasma Tank Modelling and Comparison to Measurements", IEEE Trans. Plasma Sci. **36**, 2369-2377, 2008.
10. Beattie, J.R., Williamson, W.S., Matossian J.N., Vourgourakis E.J. and Burch, J. L., AIAA-1989-1603 "High-current Plasma Contactor Neutralizer System," 3rd International Conference on Tethers in Space - Toward Flight, San Francisco, CA, May 17-19, 1989.
11. Parks, D.E., Katz, I., Buchholtz, B. and Wilbur, P.J, "Expansion and Electron Emission Characteristics of a Hollow-cathode Plasma Contactor," J. of Appl. Phys. **74**, 7094-7100, 1993.
12. Williams, J.D. and Beattie, J.R., "Spacecraft Potential Control using Plasma Contactors," 3rd International Workshop on the Interrelationship Between Plasma Experiments in the Laboratory and in Space, IPELS'94, Pitlochry, Scotland, July 24-28, 1994.
13. Capel, A., O'Sullivan, D. and Marpinard, J.C., "High-power Conditioning for Space Applications". IEEE Proceedings **76**, 391-408, 1988.
14. Weinberg, A.H. and Ghislanzoni, L., "A New Zero Voltage and Zero Current Power Switching Technique", IEEE Trans. Power Electronics **7**, 655-665, 1992.
15. O'Sullivan, D., "Space Power Electronics - design drivers", ESA Journal **18**, 1-23, 1994.
16. Janhunen, P. *et al*, "Electric Solar Wind Sail: Towards Test Missions", Rev. Sci. Instrum. **81**, 111301, 2010.
17. "GEMS – A Mole to Explore the Interior of Mars", 12.09.2011 http://www.dlr.de/dlr/en/desktopdefault.aspx/tabid-10333/623_read-818/ .
18. Leslie Curtis, Jason Vaughn, Ken Welzyn and Joe Carroll, "Development of the flight tether for ProSEDS", Space Technology and Applications International Forum (STAIF), 3-6, 2002.
19. Fujii, H. *et al,* "Space Demonstration of Bare Electrodynamic Tape-Tether Technology on the Sounding Rocket S520-25", AIAA 2011-6503, 8-11 August 2011, Portland, Oregon.